JAREE (year), page no
doi: 10.12962/jaree.xyzxyz

Journal on Advanced Research in Electrical Engineering
ISSN: 2579-6216

RESEARCH ARTICLE

A 3x3 Phased Array Antenna for Ground Station Application

Hidayah[1], Gamantyo Hendrantoro*, Wahyudi Hashi[2], and Fannush Shofi Akbar[3]

[1] Department of Electrical Engineering, Institut Teknologi Sepuluh Nopember, Surabaya, Indonesia
[2] Research Centre for Satellite Technology, National Research and Innovation Agency, Bogor, Indonesia
[3] Department of Telecommunication Engineering, Telkom University, Surabaya, Indonesia
*Corresponding author (gamantyo@ee.its.ac.id)

Received: 16 June 2025; **Revised:** 25 July 2025; **Accepted:** 27 July 2025

Abstract

The utilization of satellite technology has undergone rapid expansion, particularly in the domain of Low Earth Orbit (LEO) satellites. The function of ground station antennas is to provide support for mission control and data communication, which is a critical aspect of their role. However, the implementation of large reflector antennas is constrained by several factors. Primarily, the cost of manufacturing these antennas is high, and their maintenance is complex and time- consuming. Additionally, these antennas are often bulky, which can impede their portability and ease of use. This study proposes a compact, cost-effective microstrip antenna array capable of automatic tracking of LEO satellites. A 3x3 uniform rectangular array with half-wavelength spacing is designed, employing cavity-backed patch antennas and X-slot-shaped defected ground structures to enhance bandwidth and achieve circular polarization. The antenna design was developed using CST Studio Suite, while the mathematical analysis of array characteristics—such as array factor and beam steering—was conducted using MATLAB. Subsequently, a prototype was fabricated and subjected to experimental testing in an anechoic chamber. The results of the measurement process demonstrate circular polarization, a gain of 10.08 dB, and a beamwidth of 66.18° at 2.22 GHz, showing strong agreement with the simulation and analytical results. These findings substantiate the proposed antenna's viability for ground station applications in LEO satellite communication.

Keywords: ground station, low earth orbit satellite, phased array antenna, s-band frequency.

I. INTRODUCTION

Satellites operating in Low Earth Orbit (LEO) position— at an altitude ranging from 160 to 2,000 kilometers—provide distinct advantages through effective communication systems, such as reduced propagation delay, lower path loss, smaller antenna requirements, and lower power consumption. These advantages are attributable to the fact that the launch costs of such satellites are reduced due to their shorter earth-satellite links and enable more efficient system operations. This, in turn, results in lower power requirements and smaller antenna systems due to reduced path losses. The system exhibits reduced propagation delay, leading to enhanced image data quality and low latency, which is crucial for missions such as remote sensing and disaster monitoring. The development of LEO satellites in equatorial orbit continues to be a subject of ongoing research and development. This satellite type performs 14 revolutions per day, with a brief duration of approximately 8–10 minutes [1]. This short visibility imposes constraints on the volume of data that can be transmitted and necessitates rapid, reliable satellite-ground communication.

One of the primary challenges lies in the dynamic trajectory of the satellite, which continuously shifts the line- of-sight relative to the ground station. Circular polarization (CP) becomes essential in such scenarios to mitigate polarization mismatch during link acquisition and tracking [2][3]. Consequently, there is a necessity for an antenna on the ground station that can track the satellite with precision and efficiency. A prerequisite for the operation of satellite technology facilities is the capacity of the ground station to receive data and perform TT&C (Telemetry, Tracking and Commanding). To ensure precise tracking and communication, ground stations are typically equipped with large reflector antennas with mechanical steering. These reflectors facilitate the integration of control segments in the context of satellite missions. The use of these antennas has been widely implemented because their high gain and narrow beamwidth [4]. However, this type of antenna has a heavy mass, large space, increased mechanical complexity, reduced flexibility, and increased operation and maintenance costs [5]. These limitations motivate the exploration of electronically steerable alternatives, particularly phased array antennas.

The utilization of phased array antennas can be regarded as a prospective option due to their capacity for expeditious beam steering without the necessity for mechanical manipulation. These antennas are well-suited for real-time tracking of LEO satellites. Nevertheless, sustaining uniform gain and beam quality across extensive scanning angles persists as a substantial design challenge. Therefore, the antenna must generate sufficient power to produce a pencil beam pattern with adequate gain to establish stable communication links throughout the satellite's pass over the Earth's surface. In order to provide beam scanning in two angular dimensions, a planar array of transmit elements must be utilized. The position of the beam is delineated by two coordinates: azimuth and elevation. These are expressed in a spherical coordinate system.

In this context, microstrip antennas emerge as promising candidates due to their compactness, low profile, ease of fabrication, and compatibility with array configurations. A plethora of studies have previously investigated various aspects of single-feed circular polarization [6], coaxial probe feeding with X-shaped slots [7], and various DGS implementations [8][9]. These studies have demonstrated the efficacy of these methods in enhancing polarization purity, bandwidth, and gain. However, these approaches are frequently examined in isolation. To the best of our knowledge, no prior work has integrated both circular polarization and DGS within a unified microstrip phased array

How to cite: Hidayah., Hendrantoro, G., Hashi, W., & Akbar, F. S. (2026). A 3x3 Phased Array Antenna for Ground Station Application. JAREE (Journal on Advanced Research in Electrical Engineering), Volume 10 (No.1).

specifically designed for dynamic tracking of LEO satellites in equatorial orbits.

This research aims to address this gap by proposing a compact, planar phased array antenna that integrates circular polarization, DGS, and probe-feed techniques to fulfill the demands of equatorial LEO tracking systems. The antenna is designed in accordance with the method outlined in [10], and parameters such as frequency allocation [11], gain target from link budget [12], and structural efficiency are considered. The objective of this research is to realize a planar phased array antenna with circular polarization that meets the beam steering range, gain, and polarization purity requirements for LEO satellite tracking in equatorial orbit. This will be accomplished by minimizing structural complexity and enhancing efficiency compared to conventional reflector based systems.

II. DESIGN OF 3X3 PATCH ARRAY

The employment of antennas at ground stations is of paramount importance in the context of satellite communication systems, wherein they facilitate the reception and transmission of signals. The present study proposes the design of a phased array antenna with antenna elements that have slots in the patch and ground, arranged in a rectangular array configuration. The functionality of the antenna is optimized for satellite tracking, thereby demonstrating its ability to resolve azimuthal and elevation angles. In order to track the position of a satellite that is distant and moving rapidly, it is necessary to calibrate the antenna with a set of single elements to produce directional antenna characteristics.

A. Single Antenna Design

The preliminary stage of this research endeavor entails the identification of a singular element antenna capable of functioning at a frequency of 2.22 GHz as the S-band operational frequency for downlink systems, facilitating communication between satellites and ground stations [13]. A comparison simulation was conducted to evaluate the performance impact of applying cavity-supported patch antennas and X-slot DGS on a single element. In the absence of both, the antenna exhibited an S11 value of -0.76 at a frequency of 2.22 GHz, signifying that the antenna failed to meet the stipulated requirements. In the absence of the DGS, the antenna exhibited a bandwidth of 31.2 MHz indicating that the beamwidth is still narrow, a beamwidth of 89.1°, and a main lobe magnitude of 6.49 dB.

The parameters to be achieved in this design are an electrically steerable antenna with 5 dB gain, 75° HPBW, and 30° scanning range using the minimum number of elements. A number of iterations were performed from a basic design in the form of a rectangular model. Rectangular microstrip is advantageous due to the fact that it is more straightforward to fabricate and analyze. In designing a rectangular microstrip antenna, it is imperative to understand several critical parameters. The methodology employed for single-patch antennas is analogous to that of line transmission microstrip antennas [14], as delineated by equations (1) through (5). Iterative procedures are executed through the modification of the length and width parameters associated with the patch and the ground. The substrate is constrained to a size that corresponds with that of the ground.

$$Wp = \frac{c}{2fr}\sqrt{\frac{2}{\varepsilon_r+1}} \quad (1)$$

$$\varepsilon_{reff} = \frac{Er+1}{2} + \frac{Er^{-1}}{2\sqrt{1-\frac{12h}{Wp}}} \quad (2)$$

$$L_{eff} = \frac{c}{2fr\sqrt{\varepsilon_{reff}}} \quad (3)$$

$$\Delta L = 0.412h\frac{(\varepsilon_{reff}+0.3)(\frac{Wp}{h}+0.264)}{(\varepsilon_{reff}+0.258)(\frac{Wp}{h}+0.8)} \quad (4)$$

$$L_p = L_{eff} - \Delta L \quad (5)$$

where Wp is patch antenna width, εreff is permitivity effective, Leff is patch antenna effective length, ΔL is length delta, Lp is patch antenna length, c is speed of light propagation (3x10^8 m/s), fr is operational frequency (Hertz), ε_r is substrate dielectric constant (F/m), and h is substrate thickness (mm).

Conversely, the dimensions of the substrate and ground plane of the antenna are determined by equations (6) to (7).

$$Wg = xh + Wp \quad (6)$$

$$Lg = xh + Lp \quad (7)$$

where Wg is substrate/ground plane antenna width, Lg is substrate/ground plane antenna length, and x is multiplier factor (≥ 6).

The development process involves the implementation of the slot technique on a microstrip antenna patch and DGS. The implementation of a configuration comprising two sets of quadrilateral apertures, organized in a cross-shape, has the potential to augment the axial ratio, thereby inducing circular polarization and augmenting the antenna beamwidth. The determination of slot dimensions is predicated on the premise that one side is made longer than the other (equation 8).

$$2.L_{s1} + d_1 < 2.L_{s2} + d_2 \quad (8)$$

where L_{s12} is slot antenna length and d_{12} is distance between slots.

The antenna's design incorporates a substrate material known as Roger 5880; a material frequently utilized in satellite applications. Roger 5880 substrate parameters with a thickness of 1.575 millimeters, a dielectric constant of 2.2, and a loss tangent (tan code) of 0.0009. The unification design is executed through the implementation of direct coupling or coaxial probe technique. This method entails the direct connection of the antenna patch and connector by perforating the substrate from the ground. The configuration of the feeding was modified to generate circular polarization and an impedance of 50 ohms. The same excitation is used to simulate coupling, with the amplitude set to 1 and the phase shift set to 0. At the same time, measurements are taken by feeding one element into another element that is attached with a dummy load, switching them back and forth. The beam scanning capability will be affected by the fact that the feeding still uses a coaxial probe for direct feeding. Therefore, this design can be developed into an active phase.

The subsequent phase involved the use of CST Studio Suite for the purpose of simulating and optimizing the system. Simulations were performed using the Time Domain Solver and meshcells above 1 million to get a more precise design when the product is fabricated. The ensuing discussion will present the design results and antenna parameters obtained, as shown in Figure 1 and Table 1.

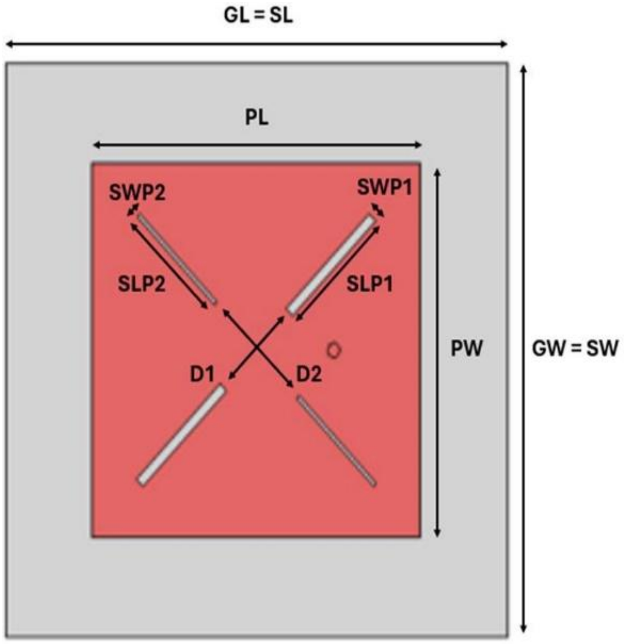

(a)

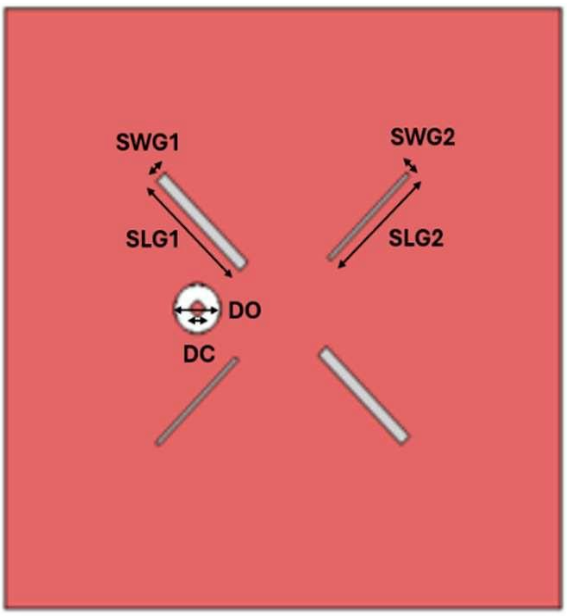

(b)

Figure 1. The optimized DGS, X-Slot patch antenna (a) Front side; (b) back side

Table 1. Optimized Antenna Design Parameters

Parameter		**Size (mm)**
Patch length = Patch width	PL = PW	40.5
Substrate length = Substrate width	SL = SW	60
Ground length = Ground width	GL = GW	60
Slot length for patch 1	SLP1	14.5
Slot width for patch 1	SWP1	1.11
Slot length for patch 2	SLP2	14.5
Slot width for patch 2	SWP2	0.5
Slot length for ground 1	SLG1	13
Slot width for ground 1	SWG1	1.25
Slot length for ground 2	SLG2	12.5
Slot width for ground 2	SWG2	0.3
Distance between slot 1	D1	11.9
Distance between slot 2	D2	14.3
Feeding diameter core	DC	0.75
Feeding diameter outer	DO	2.5

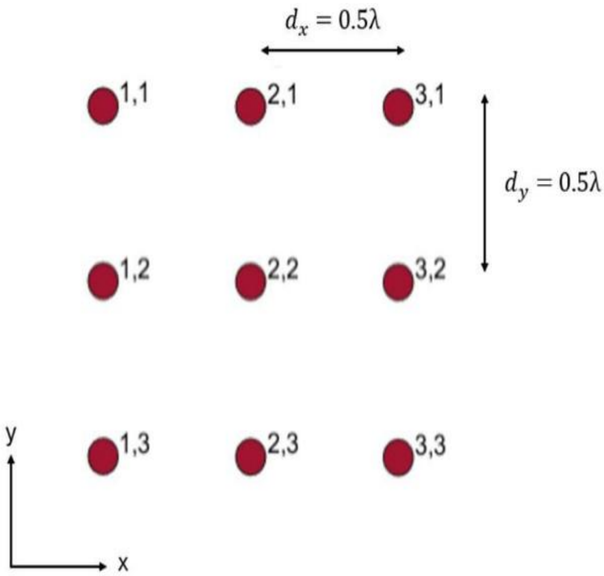

Figure 2. The element positions of 3x3 uniform rectangular array with 0.5λ spacings.

B. 3x3 Patch Array Antenna Design

Following the optimization of the single element antenna, the array size is very important for the integration of multiple antennas in handhelds. A full array is formed with the arrangement depicted in Figure 2 and 3. It is evident that each element is separated by a distance equivalent to λ/2. When the distance, d, between the elements of the array becomes greater than half a wavelength, additional beams of radiation are produced by the array. These beams are called grating lobes, and suppression of such parasitic lobes is necessary.

In this configuration, the calculation of the coupling between the elements of the antenna becomes very important, since the impedance of the elements varies as a function of the scan. A series of samples were collected from nine antenna elements to represent the overall coupling parameters.

III. Results and Discussion

Following the acquisition of the single element and array antenna designs, a comprehensive analysis of the simulation and fabrication results was conducted. The simulation results indicate the values of return loss, bandwidth, gain, side lobe level (SLL), and beamwidth. In the other hand, additional information is present in the form of mutual coupling values for the array configuration. In the analysis of fabrication results, the emphasis is placed on the mutual coupling effect that is produced.

A. Simulation Results for Single Antenna

For the optimized single-element antenna, the return loss (S_{11}) value is displayed in Figure 4. The findings indicate excellent impedance matching that the optimal S_{11} value is 20.20 dB at a frequency of 2.218 GHz. Generally, a return loss below

–10 dB is considered acceptable in the context of antenna design, as it signifies that more than 90% of the input power is transmitted into the antenna rather than being reflected. The bandwidth, defined as the frequency range where $S_{11} < -10$ dB, is 61 MHz from 2.195 to 2.256 GHz, which is sufficient for narrowband applications such as satellite communication or wireless sensors operating near 2.2 GHz.

As demonstrated in Figure 5, the Voltage Standing Wave Ratio (VSWR) value is indicated as 1.216, which is already qualified below 2. This low value indicates optimal impedance matching and negligible power reflection. Lower values of VSWR directly imply improved efficiency in power transmission from the feed to the antenna element.

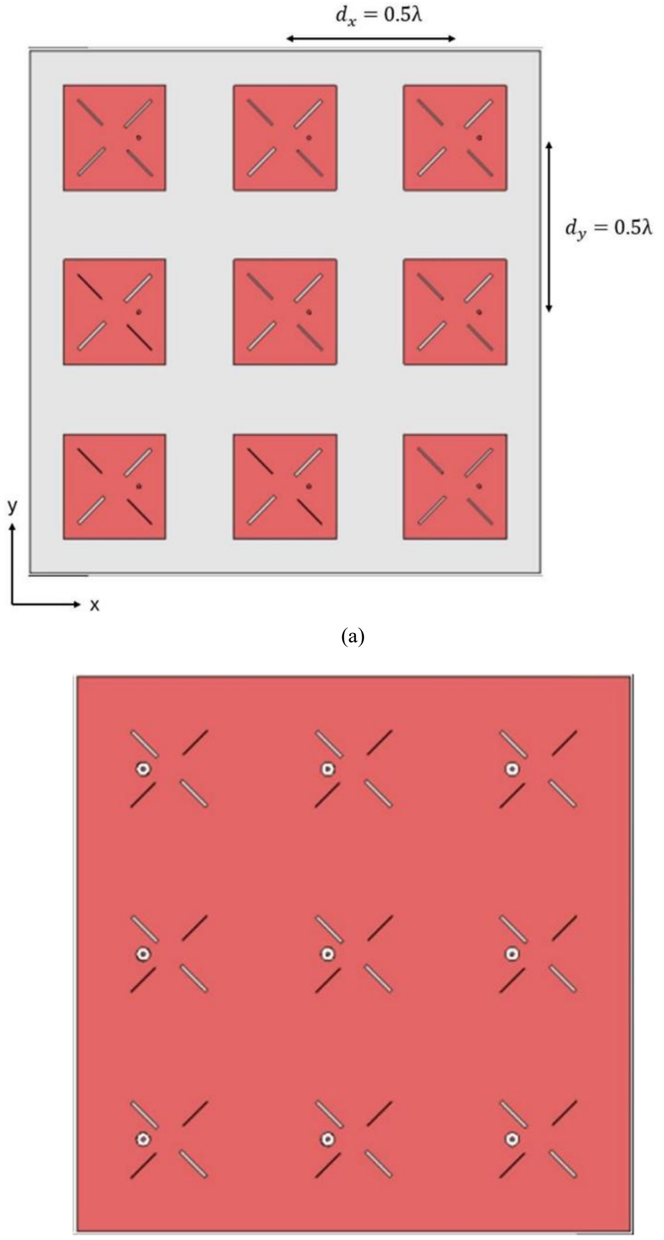

(a)

(b)

Figure 3. 3x3 patch array antenna. (a) Front side; (b) back side

As illustrated in Figure 6, the antenna exhibits a peak gain of 6.43 dB in the boresight (0°) direction, indicative of its radiation pattern. This value indicates the antenna's capacity to direct energy in a specific direction, in comparison to an isotropic radiator. In conventional single element microstrip patch configurations, gain values ranging from 5 to 7 decibels (dB) are frequently observed. This suggests that such designs attain a balanced compromise between directivity and physical size.

As illustrated in Figure 7, the 3 dB beamwidth is 86.4°, indicating a relatively wide main lobe, suitable for moderate coverage areas. The side-lobe level (SLL) of –13.3 dB is reasonably low, thereby minimizing radiation in undesirable directions and reducing the possibility of interference or multipath effects. Typically, the target SLL is set below –10 dB, thereby ensuring the effective suppression of undesired lobes.

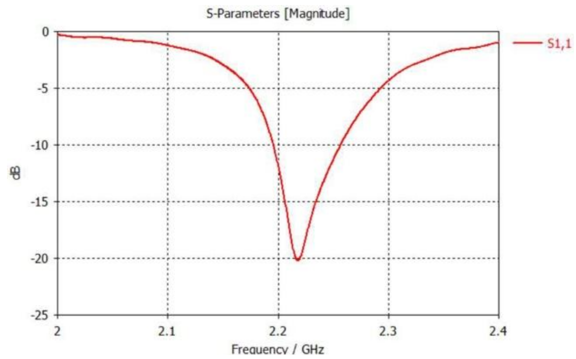

Figure 4. Return Loss for optimized single element antenna.

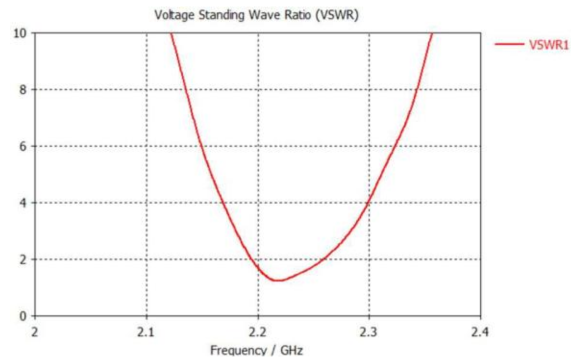

Figure 5. VSWR for the optimized single element antenna.

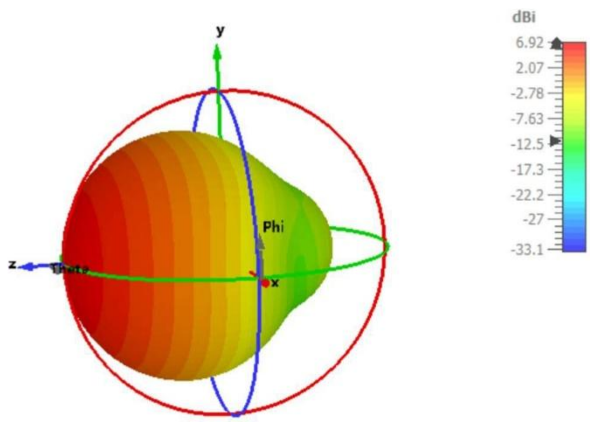

Figure 6. Gain for the optimized single element antenna.

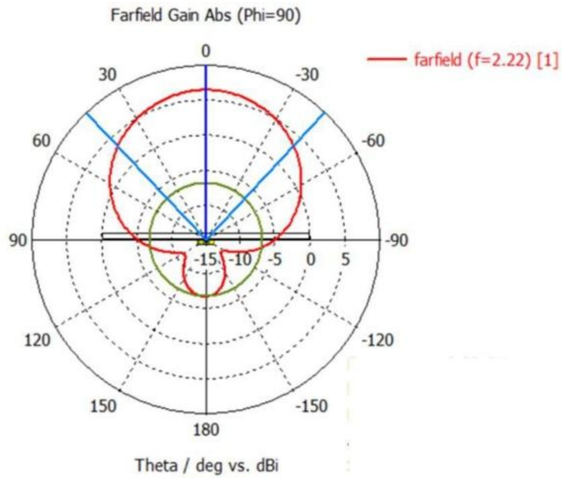

Figure 7. SLL and beamwidth for the optimized single element antenna.

Additionally, the antenna's design is optimized for circular polarization, as evidenced by an axial ratio (AR) of 2.54 as shown in Figure 8. This value falls below the established threshold of 3 dB, indicating that the antenna performs optimally within this range. A low AR guarantees that the antenna sustains polarization purity, a vital consideration for satellite communication and RFID applications, where polarization mismatch can lead to substantial signal degradation. The achieved value indicates that the antenna emits a high-quality circularly polarized wave.

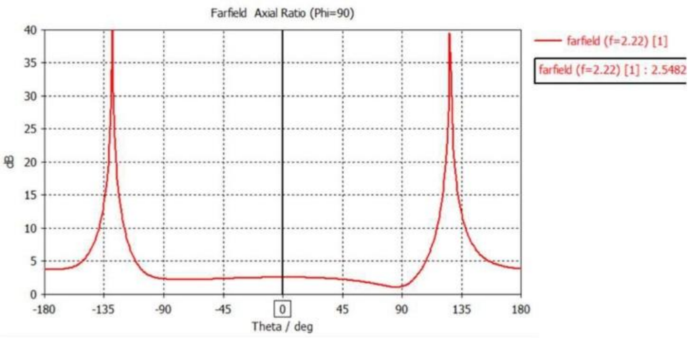

Figure 8. Axial ratio for the optimized single element antenna.

B. *Simulation Results for 3x3 Patch Array Antenna*

Following the attainment of the optimal single element design, the subsequent step involves the arrangement of said design into an antenna array. It is imperative to deliberate on the repercussions of element spacing in a 3x3 array on mutual coupling and return loss within the comprehensive array configuration. Excessive coupling between elements has been shown to degrade the impedance match and introduce pattern distortion. In the subsequent array configuration, proper inter-element spacing, typically 0.5λ, is implemented to minimize mutual coupling. This helps retain good S_{11} characteristics and array integrity.

The return loss value for 3x3 patch array antenna is displayed in Figure 9. A general observation of the graphs reveals that they exhibit nearly identical values for all nine antennas. At a frequency of 2.22 GHz, the minimum value is observed at antenna (3,3) with -33.49 dB, while the maximum value is recorded at antenna (1,1) with -26.17 dB.

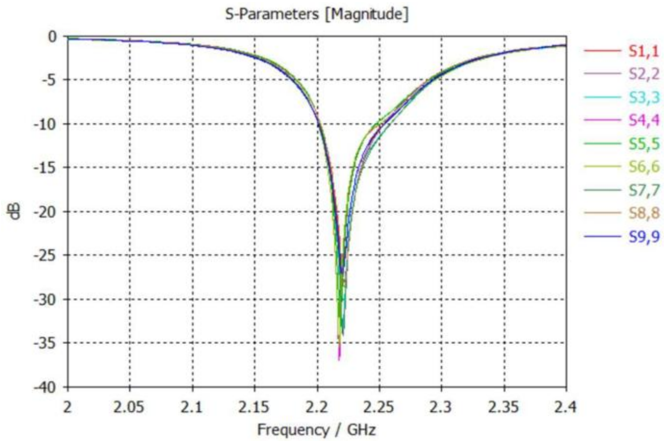

Figure 9. Return Loss for the 3x3 patch array antenna.

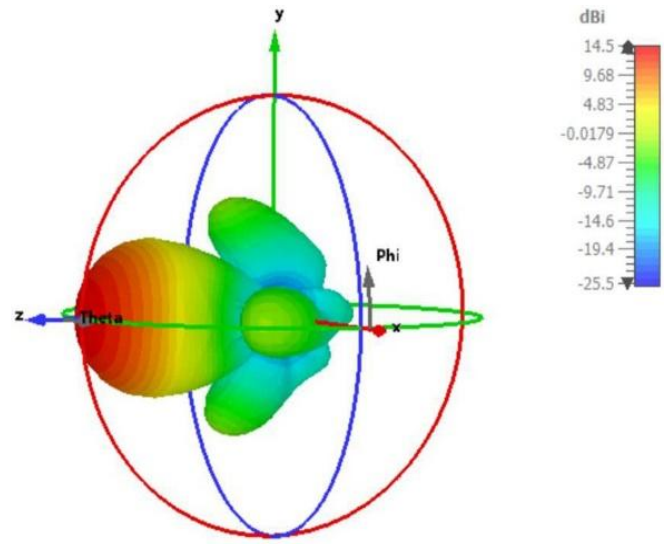

Figure 10. Gain for the 3x3 patch array antenna.

The far field value, defined as the radiation pattern on the antenna, is illustrated in Figure 10. The results indicate a gain value of 14.5 dB in the 0° direction. As illustrated in Figure 11, the side lobe level value is -16.3 dB, with an angular width (3 dB) of 33.4°. However, the evaluation of the axial ratio, which indicates circular polarization, was not performed due to equipment limitations. Figure 12 illustrates that the maximum mutual coupling value is achieved at $S_{31,21}$ with 16.51 dB, whereas the minimum value is generated by $S_{32,13}$ at 48.90 dB.

C. *Fabrication Results for 3x3 Patch Array Antenna*

The subsequent phase of the simulated array design is the fabrication stage, as illustrated in Figure 13. This stage involves the measurement of various parameters. Measurements were performed in an anechoic chamber, which is a room that is designed to minimize external noise.

The return loss (S_{11}, S_{22}, S_{33}, S_{44}, S_{SS}, S_{66}, S_{77}, S_{88}, S_{99}) value for the fabrication of 3x3 patch array antenna is displayed in Figure 14. A general observation of the graphs reveals that they exhibit nearly identical values for all nine antennas. At a frequency of 2.22 GHz, the minimum value is observed at antenna (1,1) with -16.9 dB, while the maximum value is recorded at antenna (2,2) with -11.09 dB in the 0° direction.

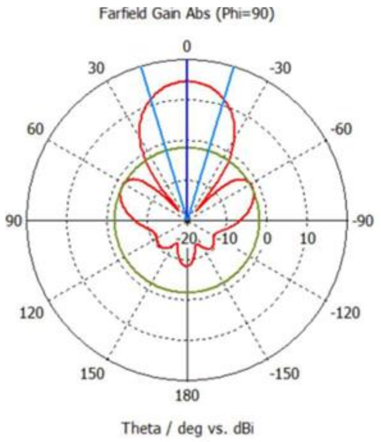

Figure 11. SLL and beamwidth for the 3x3 patch array antenna.

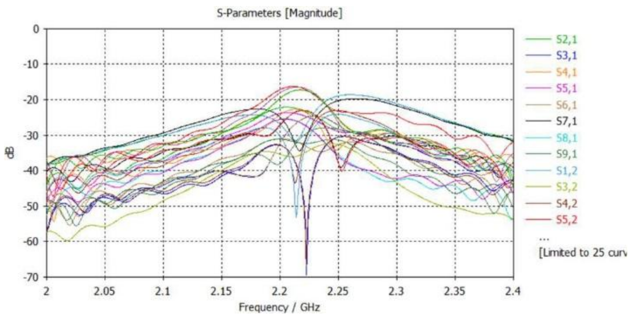

Figure 12. Mutual coupling for the 3x3 patch array antenna.

Meanwhile, the radiation pattern on the antenna is illustrated in Figure 15. The results indicate a gain value of 10.06 dB with 40° of beamwidth. The discrepancy in gain between simulation and fabrication is substantial. This can be influenced by several factors, including a less precise antenna manufacturing process, connector losses, substrate tolerances, measurement offsets, or impedance mismatches.

Another objective of this measurement is to evaluate the impact of mutual interaction between elements. The parameters selected for analysis are antennas S11, S12, S21, and S22. This selection is predicated on the position of the elements that can be utilized as a reference for the position of other elements. For instance, element S11 occupies the same position as elements S13, S31, and S33, all of which are situated at the extremity of the antenna and are flanked by three other elements. Element S12 occupies the same position as elements S21, S23, and S32, which are all situated at the center of the edge and are flanked by five additional elements. Element S22 merits scrutiny due to its central positioning within the antenna structure, with eight other elements situated on either side.

The data presented in Table 2 indicates deviations ranging from 0.5 to 13 dB. While there is a high degree of similarity between the results, it should be noted that there are some differences in the values. Furthermore, there are still some elements with mutual coupling values above -20 dB. In general, elements situated at the center of the array demonstrate superior compatibility in comparison to those located at the periphery or corners. This finding suggests that electromagnetic effects in the surrounding area and fabrication process imperfections influence the interaction between elements. However, these differences remain within acceptable limits, as the coupling values remain below -20 dB. This indicates that the isolation between elements is sufficient to support simultaneous array operation without significant interference.

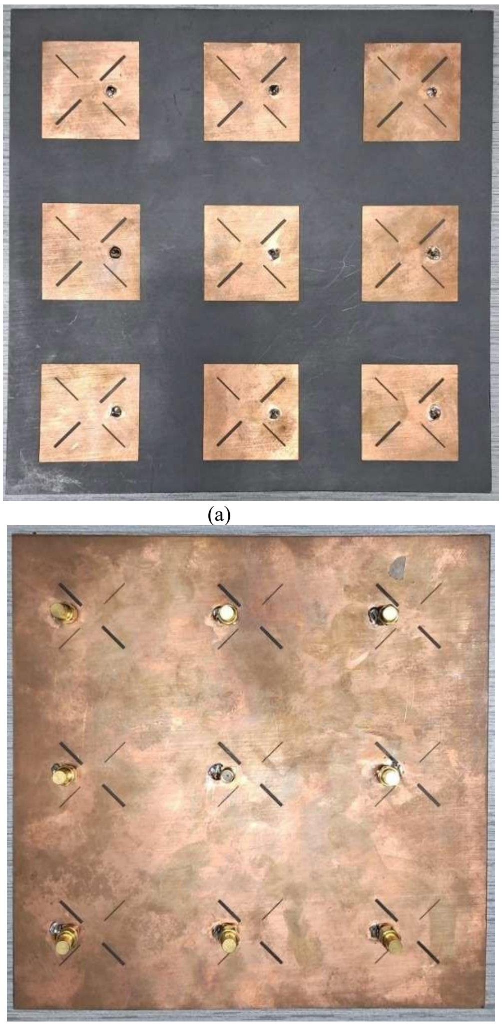

(a)

(b)

Figure 13. Fabrication for 3x3 patch array antenna. (a) Front side; (b) back side.

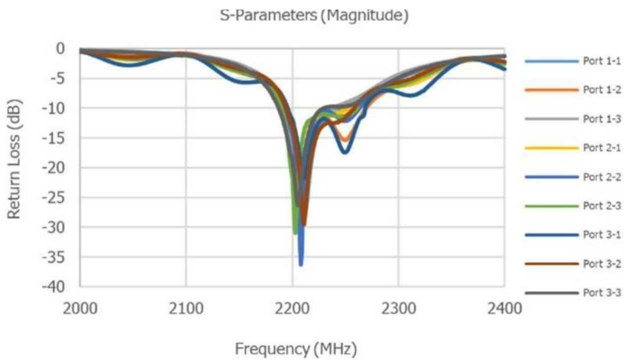

Figure 14. Return loss for fabrication of 3x3 patch array antenna.

The utilization of S-Parameter and radiation pattern data enables the simulation of the total antenna pattern through the employment of MATLAB software. As illustrated in Figure 16, the antenna exhibits the capacity to scan in both azimuth and elevation directions, with angular deviations of 0° and 30°, respectively. The results presented in Table 3 demonstrate that the decrease in gain is concomitant with an increase in SLL. This phenomenon must be taken into consideration during scanning at azimuth angles of 0° and 30°. A decrease in the HPBW is observed when scanning at elevation angles of 0° and 30°, though the effect is within typical tolerance.

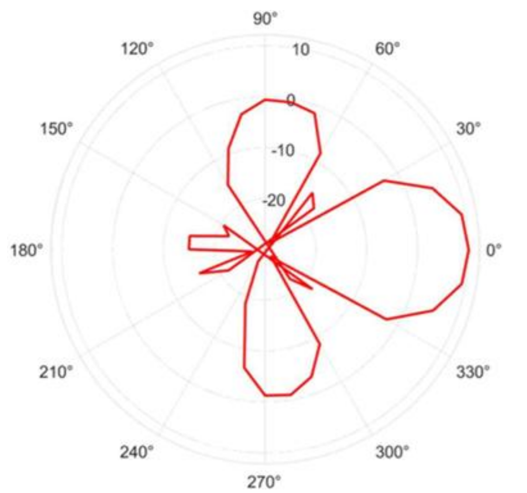

Figure 15. Radiation pattern for fabrication of 3x3 patch array antenna.

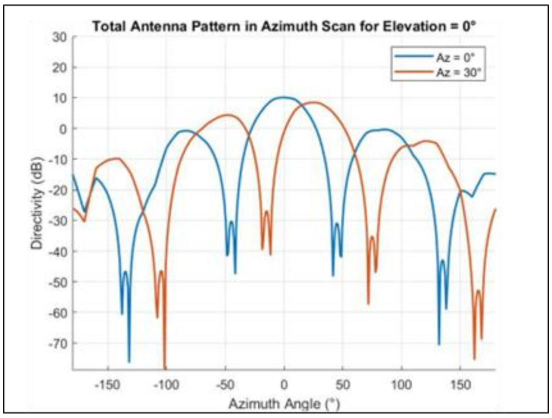

(a)

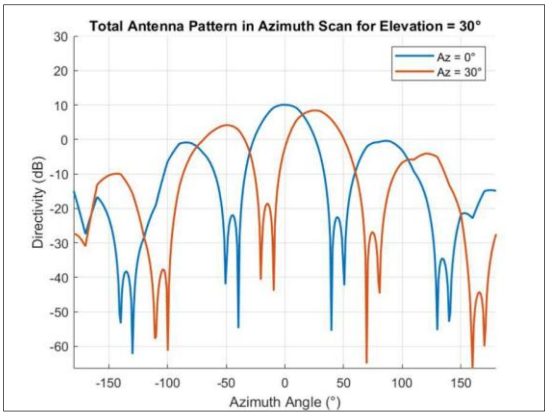

(b)

Figure 16. Comparison of total antenna pattern for azimuth angle 0° and 30°. (a) At elevation angle 0°; (b) at elevation angle 30°.

Table 2. Mutual Coupling Comparison

Element		Simulation (dB)	Fabrication (dB)
S11	S12	-28.64	-26.85
	S21	-17.27	-18.08
	S22	-24.44	-31.52
S12	S11	-28.69	-30.33
	S13	-32.77	-19.72
	S21	-33.23	-23.88
	S22	-16.75	-19.32
	S23	-22.98	-21.70
S21	S11	-17.34	-21.04
	S31	-16.63	-17.96
	S12	-33.27	-30.01
	S22	-28.72	-22.20
	S32	-23.09	-24.12
S22	S11	-24.48	-21.64
	S12	-16.88	-20.40
	S13	-35.41	-25.29
	S21	-28.70	-21.96
	S23	-28.11	-22.28
	S31	-36.39	-36.26
	S32	-16.85	-15.96
	S33	-24.66	-24.84

Table 3. Comparison Array Antenna Performance

	Elevation = 0°		Elevation = 30°	
	Azimuth = 0°	Azimuth = 30°	Azimuth = 0°	Azimuth = 30°
HPBW (°)	33.09	33.09	31.09	31.09
Gain (dB)	10.08	8.45	10.08	8.42
SLL (dB)	10.48	4.13	10.50	4.27

IV. Conclusion

The study revealed relatively small deviation between the simulation outcomes and the fabrication process. The proposed array configuration possesses the potential to serve as the foundational framework for the development of antennas at ground stations, particularly those of the phased array type. The objective is to achieve superior benefits in comparison with those attained by the utilization of large- diameter antennas.

The simulation results of single-element antenna indicate an increase in gain of 6.43 dB, accompanied by 86.4° of HPBW at a working frequency of 2.22 GHz. The optimization of design can be accomplished through the incorporation of size parameters, encompassing the dimensions of the slots in the patch and ground, as well as the position of the union. Furthermore, modifications to the techniques employed can be applied to maximize antenna performance. The results obtained from this process are subsequently employed in a more comprehensive array. It has been demonstrated that the examination of arrays of odd sizes is less arduous due to the presence of a center point those functions as a performance reference point for the elements in its vicinity. The desired results are quite robust with the application of a uniform rectangular array with λ/2 spaced in the antenna design used. The utilization of a substantial quantity of elements is the pivotal factor in determining the gain value of 10.08 dB and the beamwidth of 66.18°.

The employment of this specific antenna configuration is rendered technically viable by the strategic implementation of an economically advantageous microstrip-type antenna in the manufacturing process. Furthermore, the substrate material, which is characterized as Roger 5880, has been demonstrated to facilitate high-frequency communication with an expanded bandwidth capacity. This array configuration produces high gain values for LEO (Low Earth Orbit) satellite tracking at azimuth and elevation angles suitable for efficient data transmission from high-capacity, high-speed satellite payloads. This research provides a foundation for future innovations in the field of antenna design and optimization for satellite communication applications. It offers appropriate technical solutions and lays the groundwork for subsequent advancements in the realm of satellite communication. Therefore, the objective is to obtain the antenna specifications necessary to track LEO satellites.

Acknowledgment

The reported research was carried out during a placement of Hidayah at Research Centre for Satellite Technology by National Research and Innocation Agency via the scheme of Degree by Reseach Scholarship with grant number 111/II/HK/2023.

References

[1] L. J. Ippolito Jr, “Satellite Communications Systems Engineering: Atmospheric Effects, Satellite Link Design and System Performance”, United Kingdom: John Wiley & Sons Ltd, 2008.

[2] F. E. M. Tubbal, R. Raad, K. W. Chin, “A Survey and Study of Planar Antennas for Pico-Satellite”, IEEE Access, Vol. 3, pp. 2590-2612, DOI: 10.1109/ACCESS.2015.2506577, 2015.

[3] R. Galuscak, P. Hazdra, “Circular Polarization and Polarization Losses”, 2006, Online, Available Link: https://www.researchgate.net/publication/228789667_Circular_Polarization_and_Polarization_Losses.

[4] S. D. Harsono, W. Hasbi, “Experimental Test for Receiving X-Band Data LAPAN-A3 Satellite with 5.4m Antenna Diameter”, IOP Conference Series: Earth and Environmental Science 149, DOI: 10.1088/1755-1315/149/1/012067, 2018.

[5] J. L. Volakis, “Antenna Engineering Handbook”, 4th Edition, New York: The McGraw-Hill Companies, 2007.

[6] S. S. Gao, Qi Luo, F. Zhu, “Circularly Polarized Antennas”, United Kingdom: John Wiley & Sons, Ltd., 2014.

[7] M. K. Ray, K. Mandal, N. Nasimuddin, “Low-Profile Circularly Polarized Patch Antenna with Wide 3 dB Beamwidth”, IEEE Antennas Wireless Propagation Letters, Vol. 18, No. 12, pp. 2473-2477, DOI: 10.1109/LAWP.2019.2940703, 2019.

[8] M. K. Khandelwal, B. K. Kanaujia, S. Kumar, “Defected Ground Structure: Fundamentals, Analysis, and Applications in Modern Wireless Trends”, International Journal Antennas Propagation, Vol. 2017, DOI: 10.1155/2017/2018527, 2017.

[9] M. M. Ulfah, Chairunrrisa, A. H. Wahyudi, A. Munir, “Slot and DGS Incorporation for Bandwidth Enhancement of Substrate Integrated Waveguide Antenna”, Progress in Electromagnetics Research Symposium, Vol. August 2018, pp. 1838-1841, DOI: 10.23919/PIERS.2018.8597800, 2018.

[10] F. S. Akbar., L. P. Lightart, G. Hendrantoro, I. E. Lager, “Use of Subarrays in Linear Array for Improving Wide Angular Scanning Performance”, IEEE Access, DOI: 10.1109/ACCESS.2019.2941398, 2019.

[11] Peraturan Menteri Komunikasi dan Informatika Nomor 13 Tahun 2018 tanggal 27 September 2018, Online, Available Link: https://jdih.komdigi.go.id/produk_hukum/view/id/619/t/peraturan+menteri+komunikasi+dan+informatika+nomor+13+tahun+2018+tanggal

[12] +27+september+2018.

[13] N. Ya’acob, J. Johari, M. Zolkapli, A. L. Yusof, S. S. Sarnin, N. F. Naim, “Link Budget Calculator System for Satellite Communication”, International Conferenec Electrical Electronic System Engineering, Vol. January 2018, pp. 115-119, DOI:

[14] 10.1109/ICEESE.2017.8298397, 2017.

[15] A. Akbar, E. T. Rahardjo, F. Y. Zulkifli, Z. Rainaldy, “Design of Microstrip Antenna with DGS Slot for Satellite Applications”, IEEE International Conference on Aerospace Electronics and Remote Sensing Technology, DOI: 10.1109/ICARES53960.2021.9665176, 2021.

[16] C. A. Balanis, “Antenna Theory: Analysis and Design”, 4th Edition, New York: John Wiley & Sons Inc., 2016.

[17] Hidayah, B. D. S. Atmodiharjo, G. Hendrantoro, W. Hasbi, P. H. Mukti, “Design of Phased Array Antenna for Equatorial Single LEO Satellite Ground Station”, IEEE International Conference on Aerospace Electronics and Remote Sensing Technology, DOI: 10.1109/ICARES64249.2024.10768008, 2024.

[18] W. L. Stutzman and G. A. Thiele, “Antenna Theory and Design”, 3th Edition, New York: John Wiley & Sons Inc., 2012.

[19] C. A. Balanis, “Modern Antenna Handbook”, New York: John Wiley & Sons Inc., 2008.

[20] R. J. Mailloux, “Phased Array Antenna Handbook”, 3th Edition, Artech, 2017